

## One-step Self Assemble of Cu-TiO<sub>2</sub> Heterogeneous Nanoparticles Using a Soft Template

ZHAO Peng-Jun<sup>1,2</sup>, WU Rong<sup>1</sup>, HOU Juan<sup>1,2</sup>, CHANG Ai-Min<sup>1</sup>, GUAN Fang<sup>1,2</sup>, ZHANG Bo<sup>1,2</sup>

(1. Xinjiang Key Laboratory of Electronic Information Materials and Devices, Xinjiang Technical Institute of Physics & Chemistry, Chinese Academy of Sciences, Urumqi 830011, China; 2. Graduate University of Chinese Academy of Sciences, Beijing 100049, China)

**Abstract:** Cu-TiO<sub>2</sub> heterostructure nanoparticles were successfully synthesized *via* a novel one-step self-assemble hydrothermal method using polyethylene glycol as the soft template. The nanospheres were characterized in light of the chemical composition and morphology using X-ray diffraction (XRD) and transmission electron microscope (TEM), respectively. The products are composed of cubic copper and anatase TiO<sub>2</sub>. Interfaces between Cu (101) and TiO<sub>2</sub> (111) were observed by HRTEM. In addition, the nanoparticles size could be controlled by adjusting the polymerization degrees of PEG. The accommodations of the particle sizes were mainly caused by Cu nanospheres rather than TiO<sub>2</sub>. A possible synthetic mechanism which interprets the formation of Cu-TiO<sub>2</sub> heterogeneous nanoparticles could be ascribed to the hydrogen bonds between Cu(NH<sub>3</sub>)<sub>2</sub><sup>+</sup> and PEG. UV-Vis absorption spectra indicated that the prepared product has strong absorbency in the visible region. Therefore, the unique interface nanomaterial could be used as a potential class of the materials platform as visible-light-driven photocatalyst and electrode on enhancing the photoelectric properties of solar cells.

**Key words:** Cu-TiO<sub>2</sub>; PEG; heterogeneous; hydrothermal method; visible-light absorption

TiO<sub>2</sub> materials in nanoscale have been widely used as multifunctional materials in many fields, such as the cathode of the lithium ions battery, photocatalyst, and the dye sensitized solar cells<sup>[1-10]</sup>. However, its intrinsic deficiencies limit the applications to a large degree. For one thing, the energy band of anatase is about 3.2 eV, which matches to about 400 nm at the light spectrum, implying that over 90% of solar light can not be used by pure TiO<sub>2</sub>. And recombination in large percentages of electron-hole pairs also reduces the material efficiency<sup>[11]</sup>.

Numerous contributions have been made to ameliorate the visible-light absorption as well as the photon-generated carriers' separation capacity. Doping metal or nonmetal impurities (B, N, F, Ag, Se, *etc.*) into the crystal lattice of pure TiO<sub>2</sub> is a common method to extend the spectral response range of TiO<sub>2</sub>, inducing an intermediate energy level generated between the conducting band and the valence band of TiO<sub>2</sub><sup>[12-15]</sup>. On the other hand, due to its unique architecture, TiO<sub>2</sub> nanotube is beneficial to the separation of electron-hole pairs<sup>[16-17]</sup>. Nevertheless, both the above are one-sided in improve the performance of pure TiO<sub>2</sub>.

More recently, noble metal-TiO<sub>2</sub> heterogeneous materi-

als have been found to have superior properties compared to the doping TiO<sub>2</sub> materials and TiO<sub>2</sub> nanotubes<sup>[11,18-20]</sup>. First, there are a vast number of metal-semiconductor interfaces existing in the heterogeneous materials, leading to formation of Schottky barriers between those interfaces. Because of the disparity between the metal and TiO<sub>2</sub> work function, the electrons are prone to be attracted to the surface of metal while the holes are tended to be diffused on the TiO<sub>2</sub> side. This process inhibits the recombination of electron-hole pairs. Furthermore, surface plasmon resonance of the metal in nanoscale enhances the absorption properties at visible-light. Both of them make the heterogeneous TiO<sub>2</sub> a more promising nanomaterial in many domains. Zheng, *et al*<sup>[21]</sup> prepared the noble metal-TiO<sub>2</sub> (M=Au, Pt, Ag) plasmonic photocatalysts with an *in situ* method. Au-TiO<sub>2</sub> exhibits a high catalytic activity for the oxidation of benzene to phenol in aqueous phenol. Their study has also shown that the visible-light-induced electron transfer from the Au nanoparticles to the TiO<sub>2</sub> particle during the catalytic reaction.

According to the present literatures, a two-step synthesized formation is often used to prepare the metal-TiO<sub>2</sub> nanomaterials<sup>[22-24]</sup>: firstly anamorphous precursor is ob-

Received date: 2012-03-27; Modified date: 2012-05-11; Published online: 2012-05-30

Foundation item: "Western Light Joint Scholar Foundation" Program of Chinese Academy of Sciences( LHXZ200902); China Postdoctoral Science Foundation(20100471679, 201104704)

Biography: ZHAO Peng-Jun (1986-), male, candidate of master degree. E-mail: zhaopengjun110@163.com

Corresponding author: CHANG Ai-Min, professor. E-mail: changam@ms.xjb.ac.cn

tained (step 1), then a thermal treatment at high temperatures (step 2) is carried out to form the final metal-semiconductor material. However, there are a series of drawbacks of the two step method, such as making the preparation complicated, a fairly low yield, difficult to scale-up, nonhomogeneous architectures, and so on. Moreover, using of noble metal adds costs a lot.

Herein, we introduce copper to replace the noble metal, because of the Fermi level of copper is 4.65 eV, which is between gold (5.1 eV) and silver (4.26 eV), making copper an suitable and cheap candidate to replace noble metal. In our present work, a simple one-step hydrothermal method is used to synthesize the Cu-TiO<sub>2</sub> heterogeneous nanoparticles. The formation mechanism and UV-Vis absorption performance has also been discussed in this paper.

## 1 Experimental

All reagents were analytically pure and procured from Aladdin Inc. (Shanghai), the Cu-TiO<sub>2</sub> heterogeneous nanoparticles were synthesized as the following process. Typically, 0.5 g cuprous chloride (CuCl) was dissolved in strong ammonia water to generate clathrate. Subsequently, amounts of PEG (PEG 300, 1000 and 6000) were dispersed in the mixture solution accompanied with constant magnetic stir for 5 min. After that, 10 mL absolute ethyl alcohol mixed with 0.005 mol tetrabutyl titanate (C<sub>16</sub>H<sub>36</sub>O<sub>4</sub>Ti, TBT) was added to the solution drop by drop and agitated for 15 min. Then 0.8 g ascorbic acid (C<sub>6</sub>H<sub>8</sub>O<sub>6</sub>) and 1.4 g sodium citrate (C<sub>6</sub>H<sub>5</sub>O<sub>7</sub>Na<sub>3</sub>·2H<sub>2</sub>O) were added into the solution with a strong stir about 10 min. A dark brown homogeneous liquid was obtained subsequently. Finally, 0.6 g carbamide was dissolved into the solution and maintained stirred for 20 min, the final mixture was transferred into a 50 mL Teflon-lined stainless autoclave. After 15 h hydrothermal process at 453 K and cooled to ambient temperature, the products were centrifuged using deionized water and alcohol several times to wash out of the impurities, and then dried at 333 K for future use.

The phase composition of the samples was determined by X-ray diffraction (BRUKERD8-ADVANCE, Germany) with CuK $\alpha$  radiation ( $\lambda=0.15406$  nm). The morphology of the prepared samples was investigated by Transmission Electron Microscope (TEM, Hitachi H-600, Japan). The High-Resolution Transmission Electron Microscope (HRTEM) images were taken on a JEM-2010 JEOL instrument with a tungsten filament, using an accelerating voltage of 200 kV. The corresponding Fast Fourier Transfer (FFT) patterns were obtained using the Digital Micrograph (DM) software to treat the related HRTEM images. Absorption properties of the products were recorded by TU-1901 UV-Vis Spectrophotometer (Beijing Pirkinje

General Instrument Co., Ltd).

## 2 Results and discussion

The crystalline phases of the sample added PEG 6000 is shown in Fig. 1(d). Obviously, the sample is composed of copper (Cubic phase, JCPDS 04-0836) and anatase (JCPDS 65-5714), and no peaks from other impurities can be found. The diffraction peaks at  $2\theta$  of 43.3°, 50.4° and 74.1° can be corresponded to the (111), (200) and (220) facets of cubic Cu. Three distinct peaks at 25.3°, 48.0°, and 55.1° are indexed to (101), (200), and (211) planes of the titanium dioxide (Anatase form). The XRD pattern demonstrates that the monovalent copper ions have changed to elemental copper during the hydrothermal process.

TEM image shows a narrow distribution in the range of 60–90 nm (Fig. 1(a)). The contrasts are not homogeneous in most particles. Majority of the particles show a brighter contrast in the central portion, indicating of a modestly define interface material that reveal both Cu and TiO<sub>2</sub> is combined together in the same nanoparticle.

HRTEM observation demonstrates that in the local region near Cu and anatase, the copper nanocrystallines are surrounded by quadrilateral TiO<sub>2</sub> nanocrystalline. Interplanar crystal spacing of Cu and TiO<sub>2</sub> is about 0.21 and 0.35 nm (Fig. 1(c)), which are corresponded with TiO<sub>2</sub>(101) and Cu(111) lattice planes. The corresponding Fast Fourier Transform (FFT) pattern in the inset of Fig. 1(b) represents an unclosed discrete circle, indicative of (101) crystal lattice of TiO<sub>2</sub>, and the outside Cu(111) plane is also detected. The junction region between the TiO<sub>2</sub>(101)

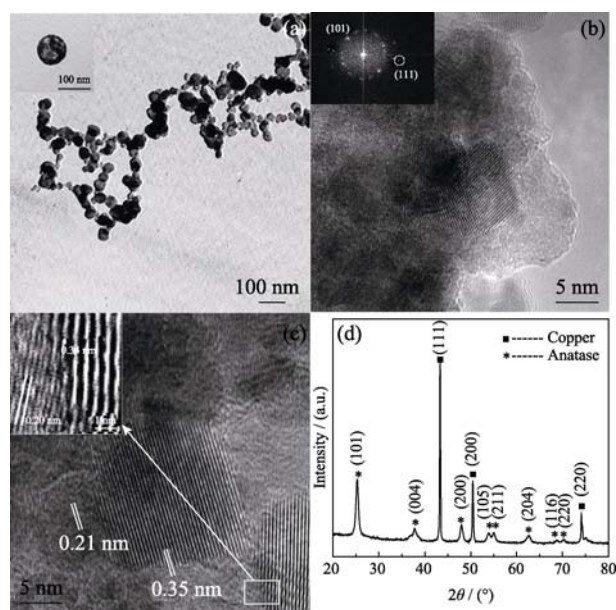


Fig. 1 TEM (a) and HRTEM (b,c) images of composite nanoparticles prepared with PEG 6000; (d) XRD pattern of composite nanoparticles prepared with PEG 6000

and the Cu(111) is presented in the inset of Fig. 1(b), different crystal structures with the lattice fringe spacing of 0.20 nm 0.34 nm are observed from the two sides of the boundary, which coincide with (111) planes of Cu and (101) planes of TiO<sub>2</sub>, as well. For Cu with narrower band gap and higher work function than individual TiO<sub>2</sub>, Schottky barriers are generated between the Cu and TiO<sub>2</sub> interfaces, which can reinforce the capability of the electron-hole pairs' separation.

Formation process of the Cu-TiO<sub>2</sub> composite nanoparticles is deemed to the following procedure, which has been schematically presented in Fig. 2(a). First, cuprous chloride (CuCl) dissolves in ammonia to generate the Cu(NH<sub>3</sub>)<sub>2</sub><sup>+</sup> complex cations. The oxygen atoms along the PEG chains tend to incorporate with the hydrogen atoms at -NH<sub>3</sub>- by the hydrogen bond<sup>[25]</sup> in the solution. The PEG-Cu(NH<sub>3</sub>)<sub>2</sub><sup>+</sup> micro balloon spheres disperse in solution and act as a soft template. Due to the high surface energy of the PEG-Cu(NH<sub>3</sub>)<sub>2</sub><sup>+</sup> spheres, amorphous TiO<sub>2</sub> or Ti(OH)<sub>4</sub> produced by hydrolyzation of Ti(OBu)<sub>4</sub> is inclined to attach to the surfaces of the PEG-Cu(NH<sub>3</sub>)<sub>2</sub><sup>+</sup> spheres; the original composite globules are generated through. After that, the added vitamin C diffuses to the inner core section of the globules and deoxidizes the

Cu(NH<sub>3</sub>)<sub>2</sub><sup>+</sup> ions to elemental copper, these Cu nanoparticles then assemble into spherical aggregates of Cu. Finally, Cu-TiO<sub>2</sub> composite nanoparticles crystallize and form the cubic copper and anatase TiO<sub>2</sub> heterostructure nanoparticles during the one-step hydrothermal process.

PEG has a specific impact on the morphology formation process. Paralleled experiments are carried out to demonstrate the formation mechanism using sample without the addition of cuprous chloride and samples with various PEG molecular weight, PEG 300 and 1000. TEM image in Fig. 2(b) shows hollow-like nanospheres in the sample without CuCl. On the basis of the interpretative formation mechanism, PEG-NH<sub>3</sub> bubbles form when CuCl is absent in the solution. TiO<sub>2</sub> hydrolyzed from TBT adheres to surfaces of the PEG-NH<sub>3</sub> bubbles, and assembles into PEG-NH<sub>3</sub>@TiO<sub>2</sub> nanospheres. PEG molecules diffuse out of the spheres during the hydrothermal process, leaving numerous TiO<sub>2</sub> hollow-like particles.

For samples with different PEG polymerized degrees of 300, 1000 and 6000, crystalline sizes of TiO<sub>2</sub> and Cu are calculated through Scherrer equation based on the XRD patterns showed in Fig. 2(c). All the samples are composed of anatase and copper. Although it seems that phase composition of the product remains the same regardless of

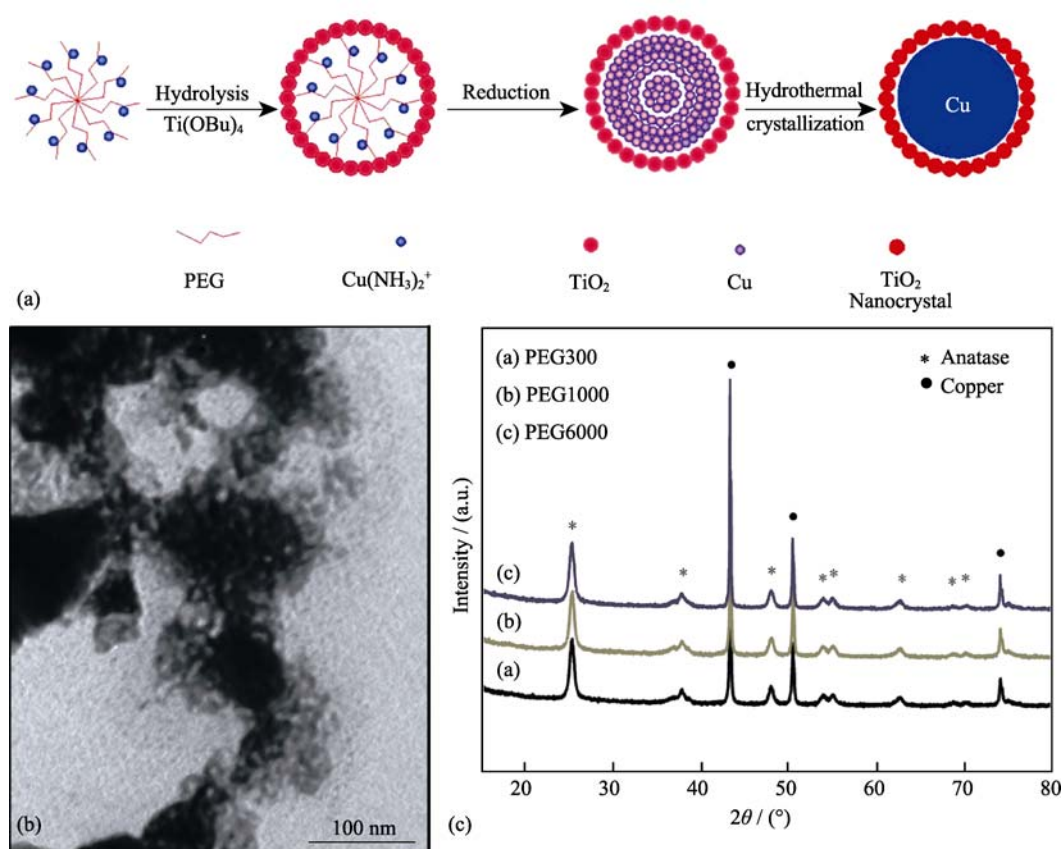


Fig. 2 (a) Schematic representation of the formation mechanism of Cu/TiO<sub>2</sub> composite; (b) TEM image of the sample prepared without CuCl; (c) XRD patterns of samples with different PEG molecular weight

PEG (formula weights 300, 1000 and 6000) is added or not, the PEG has a specific impact on the morphology formation of the crystallization process. The crystalline dimensions of  $\text{TiO}_2$  are about 14.4, 14.2 and 13.8 nm for PEG 300, 1000 and 6000, and copper of 38.9, 40.1 and 42.7 nm, which are calculated through Scherrer equation, respectively. It is revealed the grain sizes of the cubic copper grow larger as the molecular weight of PEG increases, but  $\text{TiO}_2$  are almost uniform.

Based on the formation mechanism analyzed above, crystalline sizes of copper in the heterostructure nanoparticles are dominated by the  $\text{PEG-Cu}(\text{NH}_3)_2^+$  spheres. Larger molecular weight PEG with a longer chain is capable of load more  $\text{Cu}(\text{NH}_3)_2^+$  ions. The quantity of absorbed  $\text{Cu}(\text{NH}_3)_2^+$  ions have a positive relationship with the amount of oxygen atoms of PEG. Naturally, the particle sizes of copper nanocrystalline are determined by the chain length of PEG, but the  $\text{TiO}_2$  particles are independent of this factor. Therefore, the dimensions of Cu enlarge as the increase of PEG's molecule weight, while the sizes of  $\text{TiO}_2$  for different PEG are almost the constant 14 nm.

Consequently, it is reasonable to believe that the PEG plays as the soft template during the one-step forming process. The dimension of the Cu- $\text{TiO}_2$  composite particles could be adjusted through changing the polymerization degrees of PEG. The alterations of the Cu- $\text{TiO}_2$  particle sizes are mainly caused by the Cu nanospheres rather than the  $\text{TiO}_2$ .

Ti2p XPS spectra of the as prepared sample (PEG 6000) are exhibited in Fig. 3(a). The peak at 458.6 eV is related to Ti2p<sub>2/3</sub> orbital, which is identified as the  $\text{Ti}^{4+}$  from the peak position in XPS Handbook edited by Jill Chastain<sup>[26]</sup>. However, the binding energy peak of O1s is centered at 530.3 eV (Fig. 3(b)), which is 0.3 eV shift higher than the typical binding energy of 530.0 eV. This shift in binding energy may be attributed to the existence of oxygen vacancies. The local electron density around O is lower when oxygen va-

cancies exist, which would lead to an increase of the binding energy. And in general, oxygen vacancies are beneficial to improve the performance of  $\text{TiO}_2$  photocatalyst.

The UV-Vis absorption spectra of prepared samples with different PEG molecules as well as the commercial anatase  $\text{TiO}_2$  powders (C- $\text{TiO}_2$ , from Aladdin Inc.) are shown in Fig. 4. Obviously, the samples composited with copper reveal great improvement of absorption in the visible region compared with the commercial  $\text{TiO}_2$ , and there are two absorption bands in the spectra. The strong absorption band about 320 nm is related to excitation of O2p electron to the Ti3d level, along with the broad absorption band between 350 nm and 800 nm is attributed to the emergence of Cu species, which is agreed with the former thesis<sup>[27]</sup>. For Cu with narrower band gap and higher work function than individual  $\text{TiO}_2$ , the Cu- $\text{TiO}_2$  composite particles can reinforce the capability of visible light harvest and charge carrier separation. Simultaneously, we can also identify the absorption edges of these samples from the inset of Fig. 3. All the composite samples exhibit shifts to the visible long wave at the side of C- $\text{TiO}_2$  particles, and the offset degrees are  $\text{PEG6000}$  (Fig. 4(c)) >  $\text{PEG1000}$  (Fig. 4(b)) >  $\text{PEG300}$  (Fig. 4(a)), manifesting that the particle size of the samples increases with the increase of PEG molecular weight, which is identical with the XRD observations. All the metal-semiconductor interfaces, oxygen vacancies and strong absorption at visible-light make the Cu- $\text{TiO}_2$  heterogeneous nanoparticles have potential applications on enhancing effects of photocatalysis and photoelectric properties of solar cells.

### 3 Conclusion

In summary, a novel facile one-step hydrothermal synthesis method has been developed to prepare Cu- $\text{TiO}_2$  heterogeneous nanospheres by using PEG as the soft template. The metal-semiconductor interfaces are well formed be-

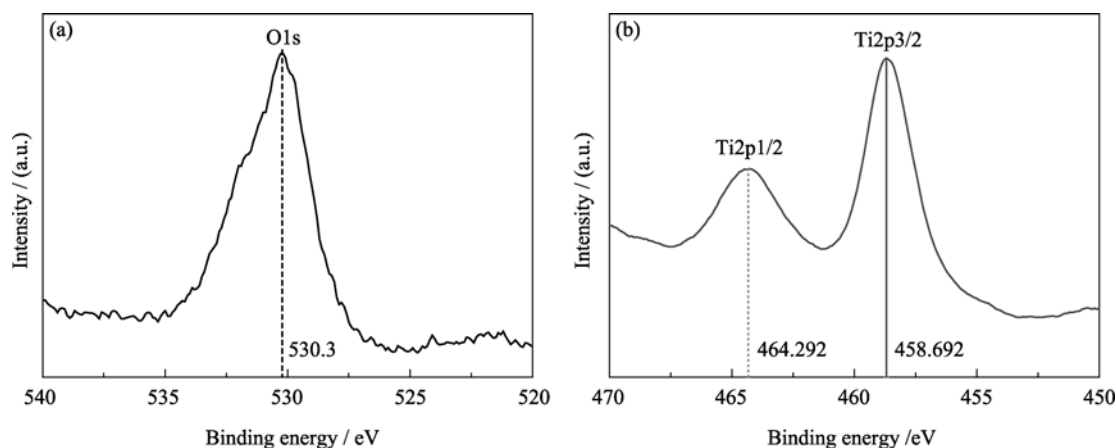


Fig. 3 XPS spectra of the sample prepared with PEG 6000

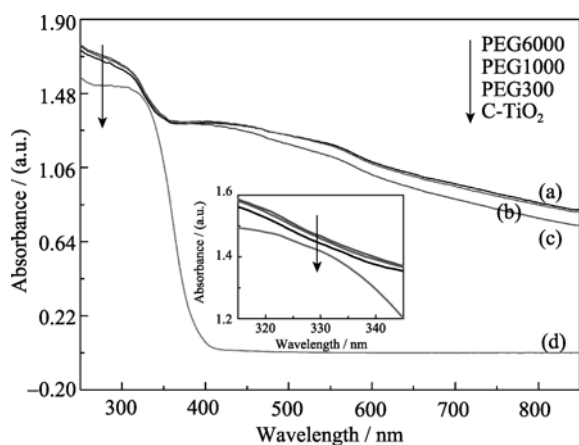


Fig. 4 UV-Vis absorption spectra of prepared samples with different PEG molecules

(a) PEG 6000; (b) PEG 1000; (c) PEG 3000; (d) Commercial anatase (C-TiO<sub>2</sub>) powders

The inset is the enlargement of the spectra in 310–350 nm

tween Cu and TiO<sub>2</sub> nanocrystals *via* TiO<sub>2</sub>(101) and Cu(111) lattice planes. The size of the composite nanoparticles can be easily tuned by controlling the average molecular weight of PEG. A plausible formation mechanism explains the phenomenon is caused by the hydrogen bonds between Cu(NH<sub>3</sub>)<sub>2</sub><sup>+</sup> and PEG. UV-Vis absorption spectra indicate the Cu-TiO<sub>2</sub> heterostructure nanoparticles have strong absorbency in the visible region compared with the commercial TiO<sub>2</sub>. The optical absorption properties can also be adjusted through altering the PEG chain length. Compared with the conventional two-step synthetic route, the new one step method is simple, low cost, environmental friendly and with the mild reaction condition. More significantly, this method may lead to a common process to prepare the metal-semiconductor composite nanoparticles with controllable sizes and optical absorption properties.

## References:

- [1] Zhang H, Yu H, Han Y, *et al.* Rutile TiO<sub>2</sub> microspheres with exposed nano-acicular single crystals for dye-sensitized solar cells. *Nano Res.*, 2011, **4**(10): 938–947.
- [2] Yella A, Lee H W, Tsao H N, *et al.* Porphyrin-sensitized solar cells with cobalt (II/III)-based redox electrolyte exceed 12 percent efficiency. *Science*, 2011, **334**(6056): 629–634.
- [3] Yoon S, Manthiram A. Hollow core-shell mesoporous TiO<sub>2</sub> spheres for lithium ion storage. *J. Phys. Chem. C*, 2011, **115**(19): 9410–9416.
- [4] Wang J, Zhou Y, Hu Y, *et al.* Facile synthesis of nanocrystalline TiO<sub>2</sub> mesoporous microspheres for lithium-ion batteries. *J. Phys. Chem. C*, 2011, **115**(5): 2529–2536.
- [5] Zhao X, Liu M, Zhu Y. Fabrication of porous TiO<sub>2</sub> film *via* hydrothermal method and its photocatalytic performances. *Thin Solid Films*, 2007, **515**(18): 7127–7134.
- [6] Zhang W, Zou L, Wang L. Photocatalytic TiO<sub>2</sub>/adsorbent nanocomposites prepared *via* wet chemical impregnation for wastewater treatment: a review. *Appl. Catal. A*, 2009, **371**(1/2): 1–9.
- [7] Li N, Liu G, Zhen C, *et al.* Battery performance and photocatalytic activity of mesoporous anatase TiO<sub>2</sub> nanospheres/graphene composites by template-free self-assembly. *Adv. Funct. Mater.*, 2011, **21**(9): 1717–1722.
- [8] Wang N, Han L, He, H, *et al.* A novel high-performance photovoltaic-thermoelectric hybrid device. *Energy Environ. Sci.*, 2011, **4**(9): 3676–3679.
- [9] Wang D, Yu B, Wang C, *et al.* A novel protocol toward perfect alignment of anodized TiO<sub>2</sub> nanotubes. *Adv. Mater.*, 2009, **21**(19): 1964–1967.
- [10] Wang H, Miyauchi M, Ishikawa Y, *et al.* Single-crystalline rutile TiO<sub>2</sub> hollow spheres: room-temperature synthesis, tailored visible-light-extinction, and effective scattering layer for quantum dot-sensitized solar cells. *J. Am. Chem. Soc.*, 2011, **133**(47): 19102–19109.
- [11] Chen X, Mao S S. Titanium dioxide nanomaterials: synthesis, properties, modifications, and applications. *Chem. Rev.*, 2007, **107**(7): 2891–2959.
- [12] Jung H G, Yoon C S, Prakash J, *et al.* Mesoporous anatase TiO<sub>2</sub> with high surface area and controllable pore size by F ion doping: applications for high-power Li-ion battery anode. *J. Phys. Chem. C*, 2009, **113**(50): 21258–21263.
- [13] Yuan J, Wang E, Chen Y, *et al.* Doping mode, band structure and photocatalytic mechanism of B–N-codoped TiO<sub>2</sub>. *Appl. Surf. Sci.*, 2011, **257**(16): 7335–7342.
- [14] Liu G, Wang X, Chen Z, *et al.* The role of crystal phase in determining photocatalytic activity of nitrogen doped TiO<sub>2</sub>. *J. Colloid Interface Sci.*, 2009, **329**(2): 331–338.
- [15] Zhen J W, Bhattacharyya A, Wu P, *et al.* The origin of visible light absorption in chalcogen element (S, Se, and Te)-doped anatase TiO<sub>2</sub> photocatalysts. *J. Phys. Chem. C*, 2010, **114**(15): 7063–7069.
- [16] Wang D, Liu Y, Wang C, *et al.* Highly flexible coaxial nanohybrids made from porous TiO<sub>2</sub> nanotubes. *ACS Nano*, 2009, **3**(5): 1249–1257.
- [17] Wang Q, Zhu K, Reale N R, *et al.* Constructing ordered sensitized heterojunctions: bottom-up electrochemical synthesis of p-type semiconductors in oriented n-TiO<sub>2</sub> nanotube arrays. *Nano Lett.*, 2009, **9**(2): 806–813.
- [18] Tanabe I, Matsubara K, Sakai N, *et al.* Photoelectrochemical and optical behavior of single upright Ag nanoplates on a TiO<sub>2</sub> film. *J. Phys. Chem. C*, 2011, **115**(5): 1695–1701.
- [19] Wu X F, Song H Y, Yoon J M, *et al.* Synthesis of core-shell

- Au@TiO<sub>2</sub> nanoparticles with truncated wedge-shaped morphology and their photocatalytic properties. *Langmuir*, 2009, **25**(11): 6438–6447.
- [20] Park W Y, Kim G H, Seok J Y, *et al.* A Pt/TiO<sub>2</sub>/Ti Schottky-type selection diode for alleviating the sneak current in resistance switching memory arrays. *Nanotechnology*, 2010, **21**(19): 195201–1–5.
- [21] Zheng Z, Huang B, Qin X, *et al.* Facile *in situ* synthesis of visible-light plasmonic photocatalysts M@TiO<sub>2</sub> (M = Au, Pt, Ag) and evaluation of their photocatalytic oxidation of benzene to phenol. *J. Mater. Chem.*, 2011, **21**: 9079–9087.
- [22] Zhang L, Xia D, Shen Q. Synthesis and characterization of Ag@TiO<sub>2</sub> core-shell nanoparticles and TiO<sub>2</sub> nanobubbles. *J. Nanopart. Res.*, 2006, **8**(1): 23–28.
- [23] Feng C, Zhang J, Lang R, *et al.* Unusual photo-induced adsorption-desorption behavior of propylene on Ag/TiO<sub>2</sub> nanotube under visible light irradiation. *Appl. Surf. Sci.*, 2011, **257**(6): 1864–1870.
- [24] Sun Y H, Zhang M, Dong F, *et al.* Effect of Cl<sup>-</sup> anions on photocatalytic decomposition of gaseous ozone over Au@Ag/TiO<sub>2</sub> catalyst. *Res. Chem. Intermed.*, 2009, **35**(6/7): 817–826.
- [25] Cui Y, Liu L, Li B, *et al.* Fabrication of tunable core-shell structured TiO<sub>2</sub> mesoporous microspheres using linear polymer polyethylene glycol as templates. *J. Phys. Chem. C*, 2010, **114**(6): 2434–2439.
- [26] Chastain J, Moulder J F, Stickley W F, *et al.* Handbook of X-ray Photoelectron Spectroscopy. Perkin-Elmer Corporation. 1992: 44–45, 72–74.
- [27] Xu S, Ng J, Zhang X, *et al.* Fabrication and comparison of highly efficient Cu incorporated TiO<sub>2</sub> photocatalyst for hydrogen generation from water. *Int. J. Hydrogen. Energy*, 2010, **35**(11): 5254–5261.

## 一步水热模板法制备 Cu-TiO<sub>2</sub> 异质结构纳米粒子

赵鹏君<sup>1,2</sup>, 吴荣<sup>1</sup>, 侯娟<sup>1,2</sup>, 常爱民<sup>1</sup>, 关芳<sup>1,2</sup>, 张博<sup>1,2</sup>

(1. 中国科学院 新疆理化技术研究所, 新疆电子信息材料与器件重点实验室, 乌鲁木齐 830011; 2. 中国科学院 研究生院, 北京 100049)

**摘要:** 以聚乙二醇(PEG)为软模板剂, 采用一步水热法合成了具有异质结构的铜-二氧化钛复合纳米粒子. 利用 X 射线衍射谱(XRD)、透射电子显微镜(TEM)等分别对制备材料的相组成、微观结构进行了研究. 结果表明, 一步水热法制备的异质纳米粒子由单一立方相铜和锐钛矿相二氧化钛组成. 高分辨透射电子显微镜(HRTEM)在单一粒子中观测到清晰的铜(101)和二氧化钛(111)晶面构成的界面. 该界面有助于二氧化钛光生电子-空穴对的分离. 同时, 所制备纳米粒子的颗粒尺寸和光吸收特性可以通过改变 PEG 分子链长进行微调. 本研究还对水热过程的反应机理进行了讨论, 结果表明: PEG 与铜氨络合物通过氢键连接, 其链长对于粒子尺寸的影响在于 PEG 对 Cu 颗粒的尺寸进行的调节, 而此过程中二氧化钛的晶粒尺寸并无明显变化. 紫外-可见吸收光谱表明该异质纳米粒子与普通二氧化钛纳米粉体相比, 对可见光区光谱有较为强烈的吸收. 该界面纳米材料是一种有潜在应用价值的光催化材料和太阳能电池材料.

**关键词:** Cu-TiO<sub>2</sub>; PEG; 异质结构; 水热; 可见光吸收

中图分类号: O643

文献标识码: A